

Pulse Deposition of Ternary Zn-Ni-X (X=Fe, SiO₂, Cd) From Sulfate Electrolytes

*Swaminatha P. Kumaraguru, Kim Hansung & Branko N. Popov,
Center for Electrochemical Engineering, Department of Chemical Engineering,
University of South Carolina, Columbia, SC*

Zn-Ni and Zn-Ni-X (X=Fe, Cd) were electrodeposited from sulfate electrolytes. By addition of Cd, Fe to a Zn-Ni bath, it is possible to control the Zn-Ni ratio and to engineer the corrosion and hydrogen permeation properties of the alloy. Pulse deposition is applied to increase the Ni content in the deposit. The effects of average current density, rotation speed of disc electrode on deposition of Zn-Ni alloys were evaluated. The mechanism of Zn-Ni-Cd alloy deposition from an alkaline bath is studied under various bath conditions. Bath analysis using a pH-concentration diagram reveals that addition of a complexing agent is essential to maintain bath stability. Introduction of low concentrations of CdSO₄ reduces the anomalous nature of the deposit. With increase in CdSO₄ content in the bath, the final deposit has a large percentage of Cd. Rotating disk electrode reveals that the deposition of Cd is under mass transfer control, while Ni deposition is under kinetic control. It is seen that at large overpotentials, the surface of the electrode is covered with hydrogen, which lowers the deposition current efficiency. By optimizing the Cd concentration in the bath, it is possible to control the amount of Ni in the final deposit.

For more information, contact:

Branko N. Popov
University of South Carolina
Center for Electrochemical Engineering
Department of Chemical Engineering
Columbia, SC 29208
803-777-7134
FAX 803-777-8265
popov@engr.sc.edu

Introduction

Zinc, by the virtue of its low standard electrode potential ($E^\circ = -0.76\text{V}$ vs. NHE) is a very active metal, which corrodes easily.¹⁻⁸ This characteristic of zinc makes it more suitable to act as a sacrificial coating on many metals and alloys with standard electrode potentials higher than zinc. The difference in electro negativities of the coating and the substrate sets as the driving force for the corrosion of the sacrificial coating under corroding conditions. Owing to the huge difference in electro negativities of Zn and Fe, rapid dissolution of Zn happens under corroding conditions. The problem of accelerated corrosion of Zn can be overcome by alloying it with another metal which will bring the standard electrode potential of the alloy much closer to the substrate metal while still remaining on the cathodic side to provide sacrificial protection.

Zn-Ni alloys possess better corrosion resistance compared to zinc and have been studied extensively for automotive applications. The co-deposition of Zn-Ni is anomalous and a higher percent of Zn is present in the final deposit. The mechanism for this preferential deposition has been discussed extensively in literature.⁷⁻⁹ Typical nickel composition in the alloy is approximately 10% and any further increase in nickel composition is based on using a higher-than-predicted Ni/Zn ratio in the bath.^{10,11} An enhancement in the nickel composition would lead to more anodic open circuit potential, which in turn will reduce the driving force for the galvanic corrosion. Also the barrier properties associated with nickel rich deposits are superior compared to other coatings.^{12,13}

In this current work we propose to increase the content of Nickel in the deposit and there by the corrosion properties of the Zn Ni alloys. In the presence of Cd, Fe it is possible to engineer the Zn Ni ratio. Also use of pulse current helps to increase the Ni content in the Zn Ni alloys. We recently developed an acid based electrodeposition process to deposit Zn-Ni-Cd ternary alloy composites, with varying proportions of cadmium (6-30 wt %) in the coating.^{14,15} However, it was observed that the deposit from the acid bath showed poor adherence and the deposit properties deteriorated with increase in concentration of CdSO_4 in the bath. To circumvent this problem an alternate alkaline bath has been developed. However, the mechanism of Zn-Ni-Cd deposition from this bath has not been studied in detail.

The objective of this study is to increase the nickel content in the Zn Ni alloy and to understand the mechanism of Zn-Ni-Cd alloy deposition from alkaline baths.

Rotating disk studies and surface characterization techniques have been used extensively to understand the Zn-Ni-Cd deposition process.

Experimental

Zn-Ni-Cd alloy deposition was carried out on mild steel foils of thickness 0.5 mm and area 50 mm × 50 mm from an alkaline bath containing different amount of NiSO₄, ZnSO₄, and CdSO₄ in the presence of (NH₄)₂SO₄. The amount of ammonium sulfate was fixed at 80g/L. pH of the bath was adjusted by adding ammonium hydroxide. NH₄OH performs dual role to acts as a complexing agent and to stabilize the solution by acting as a pH buffer. Zn-Ni and Cd deposits, which were used for comparison studies, were obtained from commercial baths obtained from SIFCO[®] selective plating. Depositions were carried out in a three electrode setup using an EG&G type 273A potentiostat/Galvanostat. Standard calomel electrode (SCE) was used as the reference electrode and a platinum mesh served as the counter electrode. All the depositions were carried out potentiostatically. The deposition substrates were subjected to a pretreatment involving mechanical polishing with alumina powder and various grades of polishing paper followed by degreasing with soap solution. The electrodeposition was carried out under ambient conditions.

Deposit Characterization: - Electrochemical characterization was carried out in a solution containing 0.5 M Na₂SO₄ + 0.5 M H₃BO₃ at a pH of 6.5 using the same three-electrode set-up that was used for electrodeposition. The morphology and composition of the alloys deposited under various conditions were studied using SEM/EDX analysis. Composition analysis was carried out by averaging the EDX data obtained by spot analysis at around 50 different points. The compositional analysis varied less than 5% in-between the different analysis.

Pulse Depositon: - Pulse current was applied by the Potentiostat /Galvanostat Model 273 (PAR). The applied pulse current and the associated potential responses were monitored using an oscilloscope (Textronix 2430 A digital oscilloscope). The peak cathodic potential at the end of t_{on} and the peak anodic potential at the end of t_{off} were recorded as E_p and E_r respectively. The average current density is defined as $t_{on}/(t_{on} + t_{off})$. The pulse period t_{on} and relaxation period t_{off} were set at 100 ms each. For the pulse reversal mode, $i_r = -0.2 i_p$ was used under all operating conditions.

Results and Discussion

Solution Chemistry of the bath: - The solution chemistry of the bath was studied by determining the equilibrium concentrations of the various species at different pH levels. The concentrations of all the electroactive species were determined by using various element balances, equilibrium conditions, and the electroneutrality condition at a specified pH. Suitable concentrations of H₂SO₄ or NaOH were used in the computation to obtain the concentration dependence as a function of pH. The calculations had two parts-region I and region II. In region I, all electroactive species are completely dissolved. In region II, Ni(OH)₂ precipitates at higher pH levels. The governing equations for the various regions are as follows:

The variables to be determined are [Ni²⁺], [Zn(OH)⁺], [Zn₂(OH)³⁺], [Ni(OH)⁺], [Cd(OH)⁺], [Cd₂(OH)³⁺], [OH⁻], [H₂O], [SO₄²⁻], [HSO₄⁻] and [H₂SO₄]_{ad}. The equations needed are

a) Element balance on Zinc, Nickel and Cadmium

$$\begin{aligned} [Zn^{2+}] + [Zn(OH)^+] + 2[Zn_2(OH)^{3+}] &= [ZnSO_4]_{ad} \\ [Ni^{2+}] + [Ni(OH)^+] &= [NiSO_4]_{ad} \\ [Cd^{2+}] + [Cd(OH)^+] + 2[Cd_2(OH)^{3+}] &= [CdSO_4]_{ad} \end{aligned}$$

b) Element balance on Sulphur

$$\begin{aligned} [HSO_4^-] + [SO_4^{2-}] &= [Na_2SO_4]_{ad} + [ZnSO_4]_{ad} \\ &+ [NiSO_4]_{ad} + [CdSO_4]_{ad} + [H_2SO_4]_{ad} \end{aligned}$$

c) Element balance on Oxygen

$$\begin{aligned} [OH^-] + [Zn(OH)^+] + [Zn_2(OH)^{3+}] + [Ni(OH)^+] + \\ [Cd(OH)^+] + [Cd_2(OH)^{3+}] + [H_2O] + 4[HSO_4^-] \\ + 4[SO_4^{2-}] &= [H_2O]_{ad} + 4[Na_2SO_4]_{ad} + 4[ZnSO_4]_{ad} \\ &+ 4[NiSO_4]_{ad} + 4[CdSO_4]_{ad} + 4[H_2SO_4]_{ad} \end{aligned}$$

d) Electroneutrality condition

$$\begin{aligned} [OH^-] + [HSO_4^-] + 2[SO_4^{2-}] &= 2[Na_2SO_4]_{ad} + [H^+] \\ + 2[Zn^{2+}] + [Zn(OH)^+] + 3[Zn_2(OH)^{3+}] &+ 2[Ni^{2+}] + \\ [Ni(OH)^+] + 2[Cd^{2+}] + [Cd(OH)^+] + 3[Cd_2(OH)^{3+}] & \end{aligned}$$

e) Equilibrium relations

$$\begin{aligned}
 [H^+][SO_4^{2-}] - K_1[HSO_4^-] &= 0 \\
 [Zn^{2+}][OH^-] - K_2[Zn(OH)^+] &= 0 \\
 [Zn^{2+}][OH^-]^3 - K_3[Zn_2(OH)^{3+}] &= 0 \\
 [Ni^{2+}][OH^-] - K_4[Ni(OH)^+] &= 0 \\
 [Cd^{2+}][OH^-] - K_5[Cd(OH)^+] &= 0 \\
 [Cd^{2+}][OH^-]^3 - K_6[Cd(OH)^{3+}] &= 0 \\
 [H^+][OH^-] - K_7 &= 0
 \end{aligned}$$

The values of the equilibrium constants are as follows: $K_1 = 1.2 \times 10^{-2} \text{ mol/cm}^3$, $K_2 = 1.1 \times 10^{-6} \text{ mol/cm}^3$, $K_3 = 5.1622 \times 10^{-8} (\text{mol/cm}^3)^3$, $K_4 = 2 \times 10^{-5} \text{ mol/cm}^3$, $K_5 = 1.1 \times 10^{-7} \text{ mol/cm}^3$, $K_6 = 5.1622 \times 10^{-8} (\text{mol/cm}^3)^3$, $K_7 = 1 \times 10^{-14} (\text{mol/cm}^3)^2$.

The above set of equations were solved using Maple®. Figure 1 presents the concentration-pH diagram for the various species. From the plot it can be seen that in acidic conditions all the species exist as bivalent cations. The concentration of monohydroxide species is negligible. As the pH increases, the concentration of bivalent cations decreases and all species exist as monohydroxides under neutral to mildly alkaline conditions. As the pH increases above 9, all species precipitate as hydroxides and the bath becomes unstable. In alkaline conditions none of the species exists in its ionic form and the concentration of the monohydroxides are again negligible. Similar results are also seen in practice. Nickel and zinc precipitate in alkaline conditions without any stabilizing agents. In our experimental studies to maintain the stability of the bath sodium citrate and ammonium hydroxide were used as complexing agents. Hence the concentration of free ionic Ni or Cd species in the bath remains low and deposition proceeds by reduction of the univalent monohydroxide ions.

Stripping cyclic voltammogram (SCV): - SCV was used to obtain preliminary information about the Zn-Ni-Cd deposition process. Electrodeposition of Zn-Ni-Cd was carried out on platinum rotating disk electrode from solution containing 1g/L of CdSO₄, 20g/L of NiSO₄, 40g/L of ZnSO₄ and 0.5M Na₂SO₄. Figure 2 shows the SCV analysis of Zn-Ni-Cd depositions obtained at different rotation speeds. The potential scan of the SCV began at -0.4 V vs. SCE in the cathodic direction until -1.5 V after which the scan was reversed to come back to the starting point. During the cathodic scan, the deposition of Zn, Ni and Cd proceeds along with the hydrogen

evolution reaction. The deposition currents begin to increase after about -0.9 V and rises indefinitely due to accompanying hydrogen evolution reaction. During the anodic scan distinct peaks were observed which could be attributed to the dissolution of alloy components. Based on the potentials at which these peaks occur, one can make a qualitative estimate of the alloy composition. The first peak that is seen at around -0.8 V vs. SCE corresponds to the Zn dissolution.¹⁴ Based on the potential at which occurs (-0.6 V vs. SCE), the second anodic dissolution peak can be thought to be due to the dissolution of Cd rich phase. The third dissolution peak that is seen in the anodic scan of the SCV is attributed to the dissolution of Ni rich phase. When the rotation speed is increased, the Cd and Zn dissolution peaks increase indicating the mass transfer controlled nature of the deposition processes, which are in agreement with previous studies.¹⁴ Ni dissolution peak on the contrary decreases on increasing the rotations speed. Nickel deposition is kinetic controlled¹⁵ and observed decrease in nickel content in the co-deposit is merely due to the effect of accompanying side reactions that are under mass transfer control. With this knowledge about the deposition process, we next proceed to study the effect of composition of the bath on the deposit composition and properties.

Effect of Cd concentration: - Figure 3 shows the effect of CdSO_4 concentration and deposition potential on the composition of Zn-Ni-Cd ternary alloy. The concentration of CdSO_4 was varied from 0.5g/L to 3g/L while the concentration of ZnSO_4 and NiSO_4 were fixed as 10g/L and 40g/L respectively. The bath pH was maintained at 9.3 and the depositions were done without any stirring of solution. Composition analysis was performed using EDX. In case of Cd they varied between ± 1.3 and ± 1.8 . For Zn content in the alloy, the standard deviations were between ± 2.4 and ± 4.3 . The standard deviation for nickel content was estimated to be between ± 1.1 and ± 1.6 . Also, the surface concentration analyses were carried out on three different deposits obtained under similar plating conditions. The Zn, Ni, and Cd content in the alloy varied within $\pm 6.7\%$, $\pm 4.3\%$ and $\pm 5.3\%$, respectively.

As it was shown in the stripping cyclic voltammetry studies, cadmium and zinc depositions are mass transfer controlled process while nickel deposition is kinetic controlled. Due to this reason, the applied potential of electrodeposition and concentrations of the electroactive species largely affect the deposit composition and thereby the properties. When electrodeposition is carried out at potentials at -1.0V , the concentration of Cd dominated in the deposit because of its low reduction potential when compared to that of Zn. Ni also has a low

equilibrium potential but it has a high overpotential for deposition to occur. In the case of acid sulfate bath at pH 2.5, Ni deposition occurs at -0.9V vs. SCE which is much more cathodic potential than its standard potential. Further increase in the deposition potential results in an increase in the concentrations of Zn and Ni in the deposit. When CdSO_4 concentration in the bath is increased beyond 2 g/L , deposition of Zn is completely suppressed and there is a complete domination of Cd in the deposit. For better understanding of the deposition process, the partial current densities of each component were calculated using Faraday's law. Figure 4 shows a plot of the partial current densities of Zn, Cd and Ni as a function of electrodeposition potential. When the concentration CdSO_4 in the bath is $\leq 1\text{ g/L}$, increasing applied potential has an effect on the composition of the deposits because the limiting current of Cd is lower than the partial current density of Ni. Since Cd deposition is mass transfer controlled, the concentration of Cd in the deposit does not increase after once the limiting current density for deposition is reached. However, further increase in the concentration of CdSO_4 lead to an increase in the limiting current density thereby resulting in a complete domination of Cd deposition. The deposits contained about 80% Cd (Figure 2) under these conditions and increasing the applied potential did little change to the deposit composition. This study indicates that the concentration of CdSO_4 is critical to maintain a proper composition of the deposit.

Effect of pH: - pH of the electrolyte determines the concentration of the electroactive species present at the interface and thereby controls the deposition potential. For this reason, pH is a very important parameter to be studied in the electrodeposition process. Figure 5 shows the effect of pH on the deposition of Zn-Ni-Cd ternary alloy as a function of deposition potential. From figures 3 and 4, we found out that Cd deposits at high concentrations at low electrodeposition potentials and the Zn, Ni concentrations begin to increase with increasing deposition potentials. When the pH of the electrolytic bath is increased, the deposition potentials are shifted to more negative values. Zn and Ni deposition in particular begin to proceed at further negative potential values. The nickel composition in the co-deposit decreases and the cadmium concentration increases with increasing pH. The composition values given in Figure 5 have been normalized based on Zn, Ni and Cd composition values and the real change in the concentration of nickel and cadmium is not clearly seen. Figure 6 shows the partial current density of Ni and Cd deposited at different pH conditions. It is seen that increasing the pH has more influence on the

Ni content compared to the other elements. The partial current density measured at -1.4V vs. SCE exhibits that the current density of Ni decreased by 66.5% with increasing pH while the partial current of Cd did not depend on pH change so much. Cadmium partial current reaches the limiting current density at around -1.2V vs. SCE and its value decreased by 6.7% with increasing pH from 9.3 to 11.3. Therefore the changes in the deposit composition as shown in Figure 5 should be viewed carefully. The actual composition of Cd may not change significantly with change in pH, but since the concentration of Ni significantly decreases with increase in pH, normalized composition of Cd increases. This pH study suggests that low pH preferable to get high Ni and low Cd composition in the deposits. Decreasing pH can also decreased current efficiency by increasing hydrogen evolution reaction.

Effect of stirring: - All the above depositions were carried out under no stirring conditions. Zn and Cd depositions are mass transfer limited processes, and therefore, stirring is bound to have a significant effect on their deposition. Fig. 7 shows partial current densities for each component with changing stirring speed. The depositions were carried out at -1.3 V from a solution containing 1 g/L of CdSO_4 , 10 g/L of ZnSO_4 and 40 g/L of NiSO_4 at a pH of 9.3. Increasing the stirring speed enhanced the concentrations of Cd in deposit and reduced Zn and Ni. This can be explained by taking into account the fact that Cd and Zn are mass transfer control and Ni is kinetic control. The decrease in the Ni content can be attributed to the mass transfer dependence of the competing proton, Zn and Cd reduction reaction. Increasing stirring speed causes more of these ions to be present near the electrode surface and enhances the reduction reaction. In the case of Cd and Zn, both are mass controlled deposition processes but Zn deposition cannot be enhanced before the limiting current density of Cd is reached, which increases with stirring speed causing a decrease in Zn deposition rate.

Effect of ZnSO_4 concentration and additives: - Zinc composition in the deposit can be improved by either decreasing the cadmium concentration (and thereby decreasing the limiting current density of Cd deposition) or by increasing the ZnSO_4 concentration. Fig. 8 shows the effect of ZnSO_4 concentration on the deposit compositions. The concentration of NiSO_4 was fixed to be 40 g/L. The deposition was carried out potentiostatically at -1.3V vs. SCE at pH 9.3 without stirring. In the case of 1g/L of CdSO_4 , increasing ZnSO_4 replaced the portion of Cd in the deposit

due to the presence of more Zn ions for deposition. Cd concentration decreased to the point of 17% and Ni content did not change much. However when the CdSO₄ in the bath is > 1 g/L, the increase in concentration of ZnSO₄ does not produce any significant results in terms of altering the deposit compositions. These results indicate that CdSO₄ concentration plays a very critical role in obtaining a required deposit composition and that it has to be maintained below 1g/L to get deposits with high Zn and Ni concentrations.

Pulse and pulse reversal plating:- Galvanostatic pulse and pulse reversal plating of Zinc – Nickel were carried out in the sulfate bath. Fig 9. Shows the zinc content in the deposits obtained by dc deposition. The Zinc content in the deposit was determined for different electrode rotation rates as a function of the applied cathodic current density. By proper choice of the current density and agitation conditions, alloy compositions were obtained between 82 % and 91 %. A maximum Zinc content is obtained for all rotation speeds. The maximum value shifts in the direction of increasing current densities as the rotation speed of the electrode increases, indicating mass transfer controlled conditions for Zn deposition. We observe similar kind of behavior for Fe Ni alloys in our earlier studies. Fig 10 shows the composition of Zn in the Zn Ni films plated on the rotating disc electrode by pc mode. The Zinc content in the deposit was determined for different rotation rates as a function of applied cathodic current density. The deposition was carried out using pulse plating with a duty cycle of 0.5 and frequency of 80 Hz. The same bath composition that was used for dc deposition was used. At lower average current densities, the Zinc deposition is under kinetic control and the Zinc content in the alloy increases with increasing current density. As shown in Fig 10, the Zinc content reaches a maximum and then decreases with increasing current density due to the hydrogen evolution being under mass transfer control. The position of the maximum observed in Fig 10 shifts to higher current density with increase in electrode rotation speed. As expected, at higher rotation speeds, the limiting current is attained at higher current densities. The peak potential E_p at high current densities increases to a sufficiently negative value so that the mass transfer limitation is a major factor determining the zinc content in the alloy causing a flattening of the Zinc content in the zinc composition profiles. During t_{off} in the pulse current mode, Zinc dissolves at the same rate as the hydrogen evolution current to maintain the zero current. In other words, the mixed potential is in

between the open circuit potential of H_2/H^+ and Zn/Zn^{2+} which is anodic to zinc, thus causing dissolution of insignificant amounts of Zinc.

Fig 11 shows the zinc dissolution versus average current density at various electrode rotation speeds for pulse reversal mode. The zinc content in the alloy is lower for pulse reversal mode compared with the zinc content in the pulse current mode. In pulse reversal mode, the anodic current ($i_r = -0.2 i_p$) during t_{off} causes some of the zinc in the alloy to dissolve. Since nickel is passivated during the anodic process in a sulfate bath, the pulse reversal mode affects the zinc dissolution mode more than nickel dissolution. As seen in Fig 3 for the pulse reversal, the zinc content in the alloy decreases with increasing rotation speeds. The pulse reversal mode yields more anodic E_r during the relaxation period compared to the pulse current mode under the same i_p . Consequently for the pulse reversal mode at high rotation speeds, the proton depletion will be less severe at the end of t_{on} . Higher concentrations of H^+ at the end of t_{on} will cause the oxidation of H_2 to occur at lower rate during t_{off} , which introduces a more anodic potential for a given i_r , which favors zinc dissolution.

The partial current efficiency for zinc increases with increasing current density and levels off at 59% to 64 %. Zinc partial current efficiency is also dependent on the electrode rotation rate. A small decrease in the zinc partial current efficiency was observed with an increase in the rotation speed from 0 to 1200 rpm due to the parasitic hydrogen evolution reaction, which is under mass transport control. Nickel partial current gradually increases with increase in the average current density, levels off at 9.5 % to 12.5 % and is independent of agitation of electrode.

Conclusion

Corrosion resistant Zn-Ni-Cd ternary alloy with higher nickel content than conventional Zn-Ni bath was synthesized using an alkaline deposition process. Electrochemical techniques were used to study the mechanism of deposition of the Zn-Ni-Cd alloy. It is seen that electrodeposition of Zn-Ni-Cd is influenced by several parameters like pH of the bath, concentrations of the active species, stirring etc. Cadmium deposition is found to be a mass transfer controlled process and is seen to dominate the entire alloy deposition process owing to its low reduction potential. At concentrations of $CdSO_4 \leq 1$ g/L, the deposits had fairly good

amount of Ni and Zn and at higher concentrations of CdSO₄ in the bath, the limiting current density of cadmium increased thereby leading to deposition of large amounts of Cd in the deposit. For 1 g/L CdSO₄ increasing ZnSO₄ concentration in the bath lead to an increase in the Zn content in the deposit. However, for 3 g/L CdSO₄ no change in deposit composition is seen with increase in ZnSO₄ content in the bath. In the case of pulse deposition, at low applied average current in the pulse current and pulse reversal mode, the Zn deposition is in the kinetic control and the increase of the polarization resistance increases the zinc content in the deposit. For the pulse current mode at low average current densities the main electrode reactions are nickel deposition and hydrogen evolution. In this region the zinc content decreases as the rotation speed increases. Limitations due to mass transfer become more important at higher average current densities. At this region, higher electrode rotation speeds correspond to the larger zinc contents in the deposit. The applied anodic current during t_{off} in the pulse reversal mode forces more anodic potentials compared with the pulse current mode, which favors the zinc dissolution. The use of pulse current and Cd, Fe helps to increase the nickel content in the alloy. Pulse deposition has been applied to ternary Zn Ni X (X= Fe, Cd) and the results will be presented in the symposia.

References

1. S. Swathirajan, *J. Electrochem. Soc.* 133 (1986): p. 671.
2. G. W. Loar, K.R. Romer, T.J. Aoe, *Surf. Finish.* 78 (1991): p. 74.
3. M.F. Mathias, T.W. Chapman, *J. Electrochem. Soc.*, 134 (1987): p. 1408.
4. M. S. Michael, M. Pushpavanam, and K. Balakrishnan, *British Corrosion Journal*, **30**, (1995): p. 317.
5. I. Kirilova, I. Ivanov, and St. Rashkov, *J. Appl. Electrochem.*, 27 (1997): p. 1380.
6. A. Brenner, "Electrodeposition of Alloys," Vol. II, Academic Press, New York (1963).
7. N. S. Grigoryan, V. N. Kudryavtsev, P. A. Zhdan, I. Y. Kolotyркиn, E. A. Volynskaya and T. A. Vagramyan, *Zasch. Met.*, 25 (1989): p. 288.
8. E. Hall, *Plat. Surf. Finish.*, 70, 11 (1983): p. 59.
9. M. Pushpavanam, S. R. Natarajan, K. Balakrishana, L. R. Sharma, , *J. Appl. Electrochem.*, 21 (1991): p. 642.
10. K. Higaashi, H. Fukushima, T. Urakawa, T. Adaniya, K. Matsudo, *J. Electrochem. Soc.*, 128 (1981): p. 2081.
11. F. Elkhatabi, M. Benballa, M. Sarret, C. Muller, *Electrochem. Acta* 44 (1999): p. 1645.
12. A. Krishniyer, M. Ramasubramanian, B. N. Popov and R. E. White, *Plat. Surf. Finish.*, 1 (1999): p. 99.
13. A. Durairajan, A. Krishniyer, B. N. Popov, B. Haran and R. E. White, *Corrosion*, 56, 3 (2000): p. 283.
14. A. Durairajan, B. Haran, R. White and B. Popov, *J. Electrochem. Soc.* 147 (2000): p. 48.
15. A. Durairajan, B. Haran, R. White and B. Popov, *J. Electrochem. Soc.* 147 (2000): p. 4507.

List of Figures

- Fig. 1 Equilibrium pH-concentration diagram for Zn, Ni and Cd
- Fig. 2 Linear sweep voltammetry of Zn-Ni-Cd film electrodeposited from electrolyte containing 1g/L of CdSO₄, 20g/L of NiSO₄, 40g/L of ZnSO₄ and 0.5M Na₂SO₄, scan rate = 30mV/s at different rotating speeds.
- Fig. 3 Effect of CdSO₄ concentration on the alloy composition as a function of the applied potential. ZnSO₄: 10g/L, NiSO₄: 40g/L, pH: 9.3 without stirring
- Fig. 4 Effect of CdSO₄ concentration on the partial current density as a function of the applied potential. ZnSO₄: 10g/L, NiSO₄: 40g/L, pH: 9.3 without stirring
- Fig. 5 Effect of pH on the composition of the deposit and current efficiency as a function of the applied potential. CdSO₄: 1g/L, ZnSO₄: 10g/L, NiSO₄: 40g/L, without stirring.
- Fig. 6 Effect of pH on the partial current density of Ni and Cd as a function of the applied potential.
- Fig. 7 Dependence of the stirring speed on the partial current density for deposition of Zn, Ni and Cd obtained from a bath of CdSO₄: 1g/L, ZnSO₄: 10g/L, NiSO₄: 40g/L at pH: 9.3.
- Fig. 8. Effect of ZnSO₄ concentration on the alloy composition and current efficiency when the concentration of CdSO₄ are 1g/L and 2g/L. NiSO₄: 40g/L, pH: 9.3, V: -1.3V vs. SCE, no stirring
- Fig 9 Composition of dc plated Zn-Ni alloy as a function of the applied current density and several rotation speeds
- Fig 10 Zinc composition profiles as a function of current density at various rotation speeds
- Fig 11 Zinc composition profiles as a function of current density at various rotation speeds

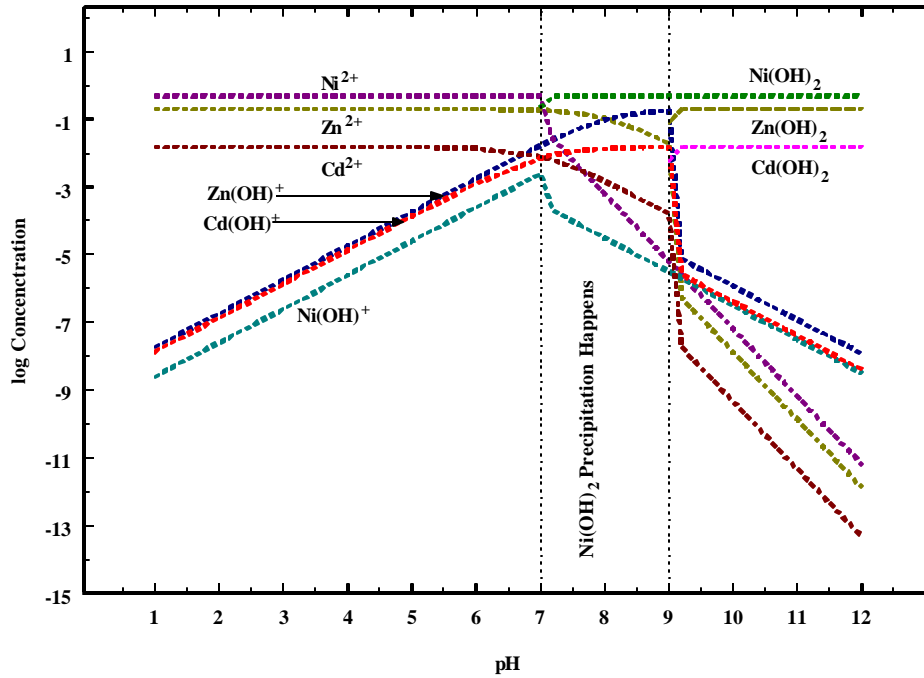


Fig. 1

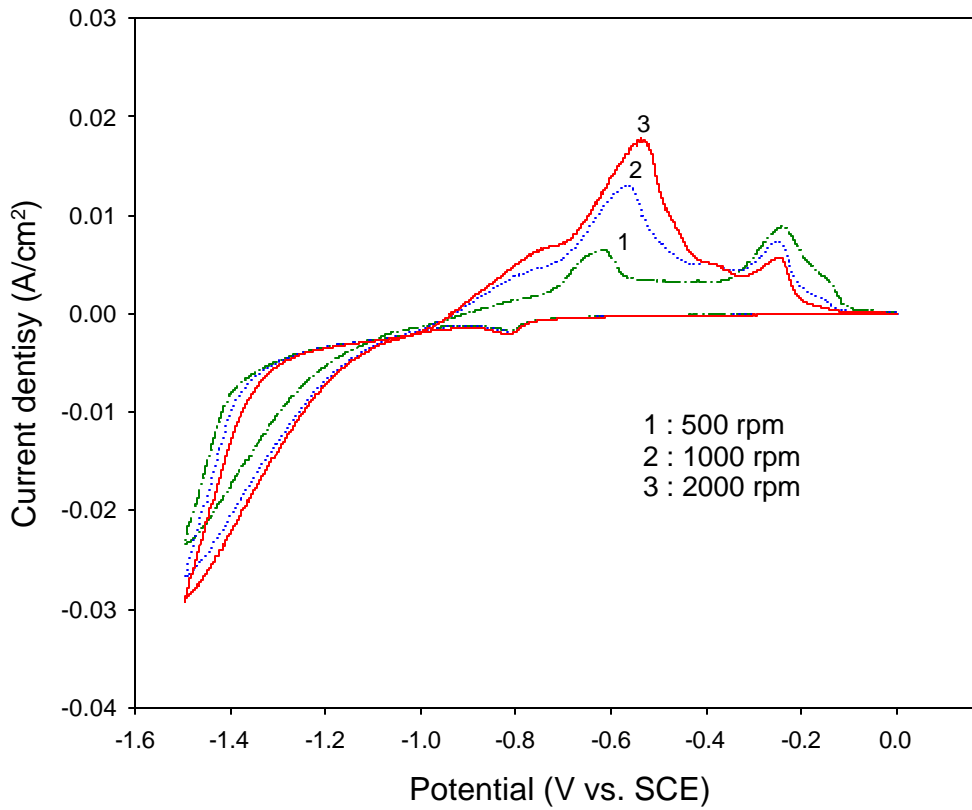


Fig. 2

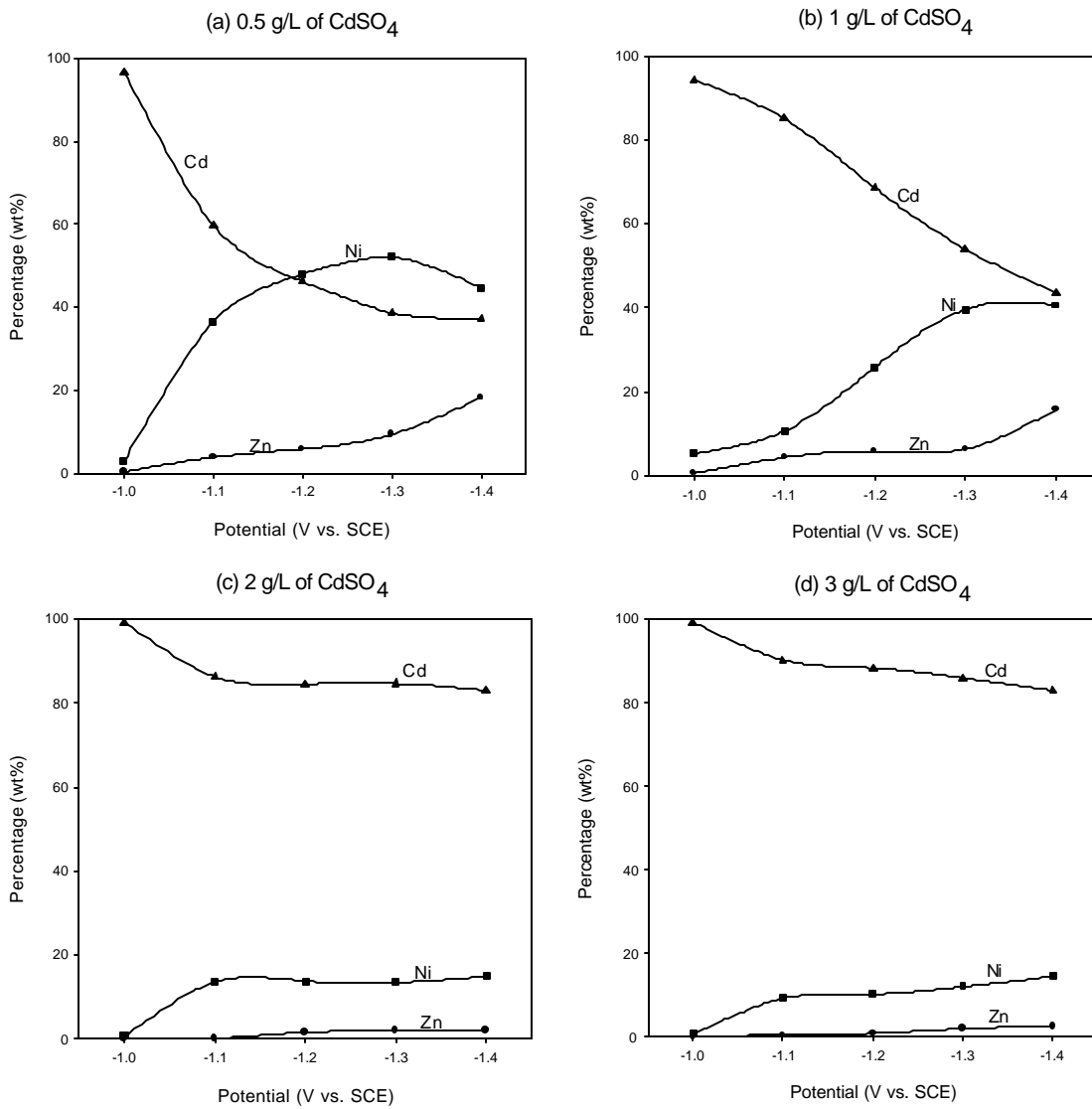


Fig. 3

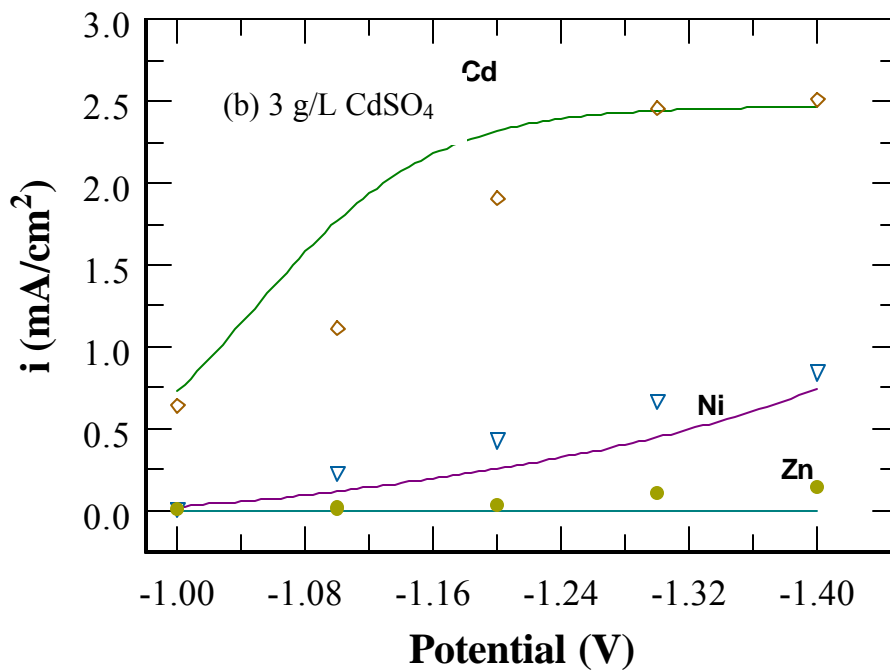
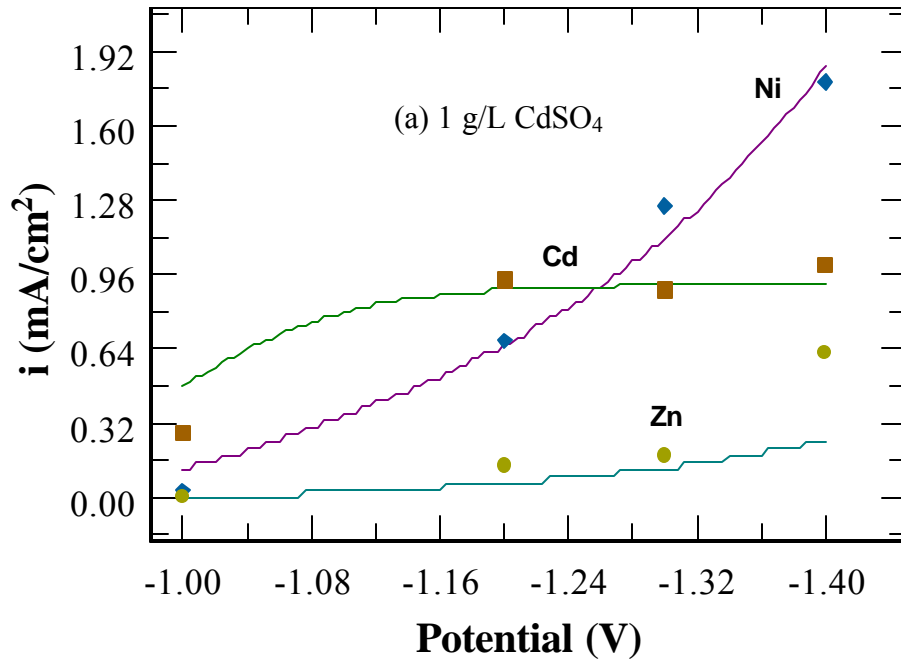


Fig. 4

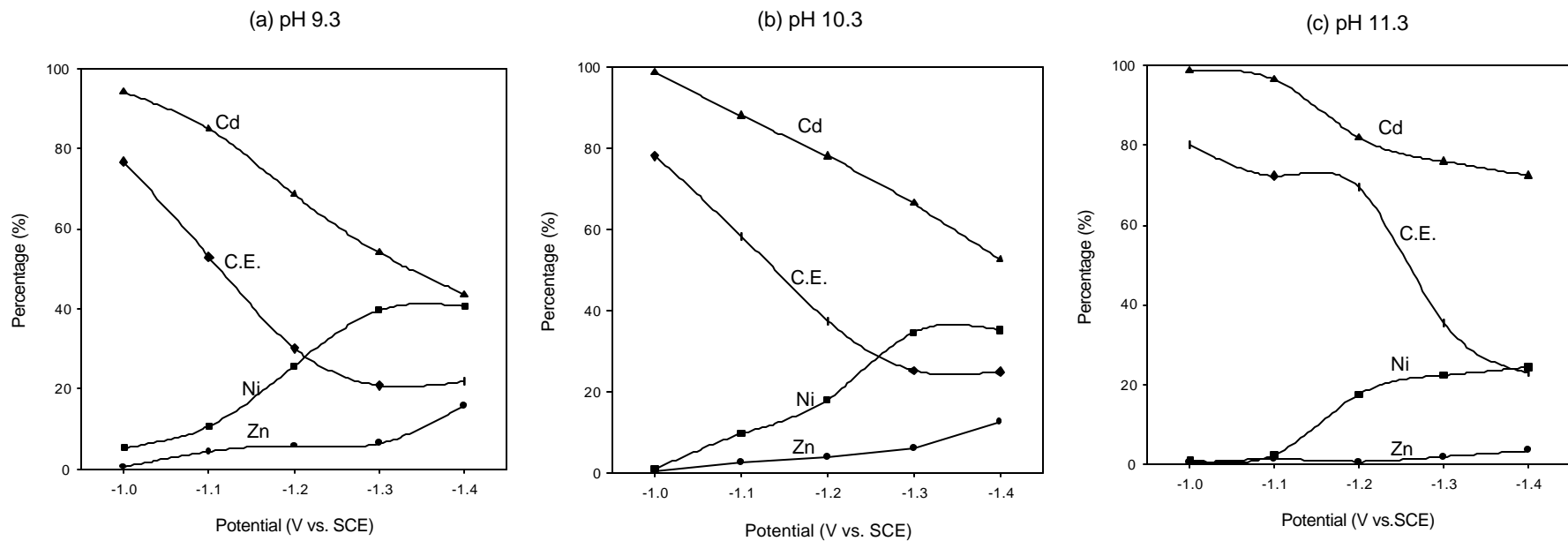


Fig. 5

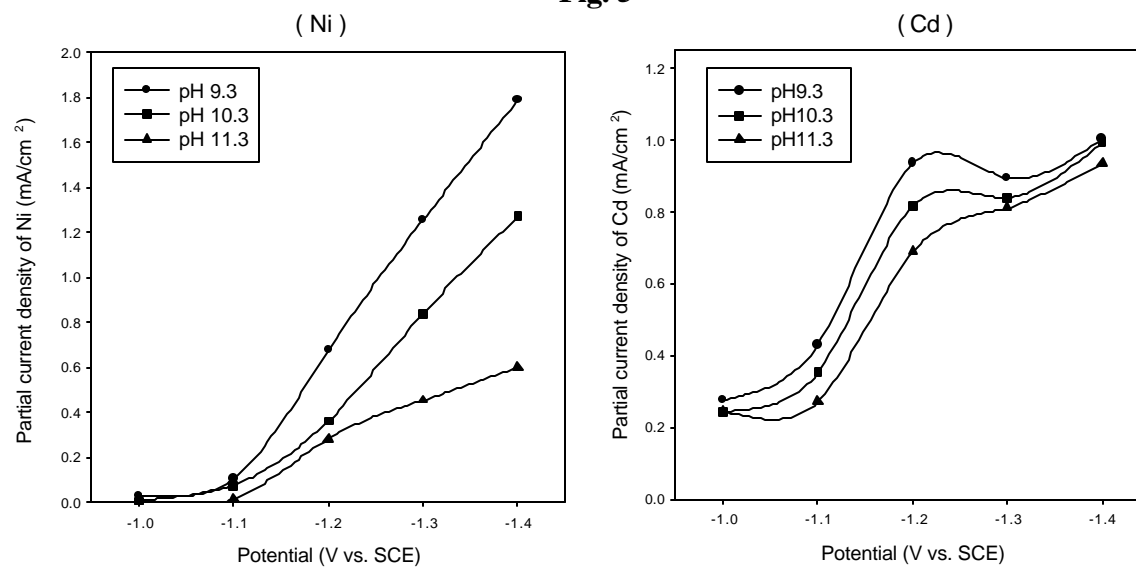


Fig. 6

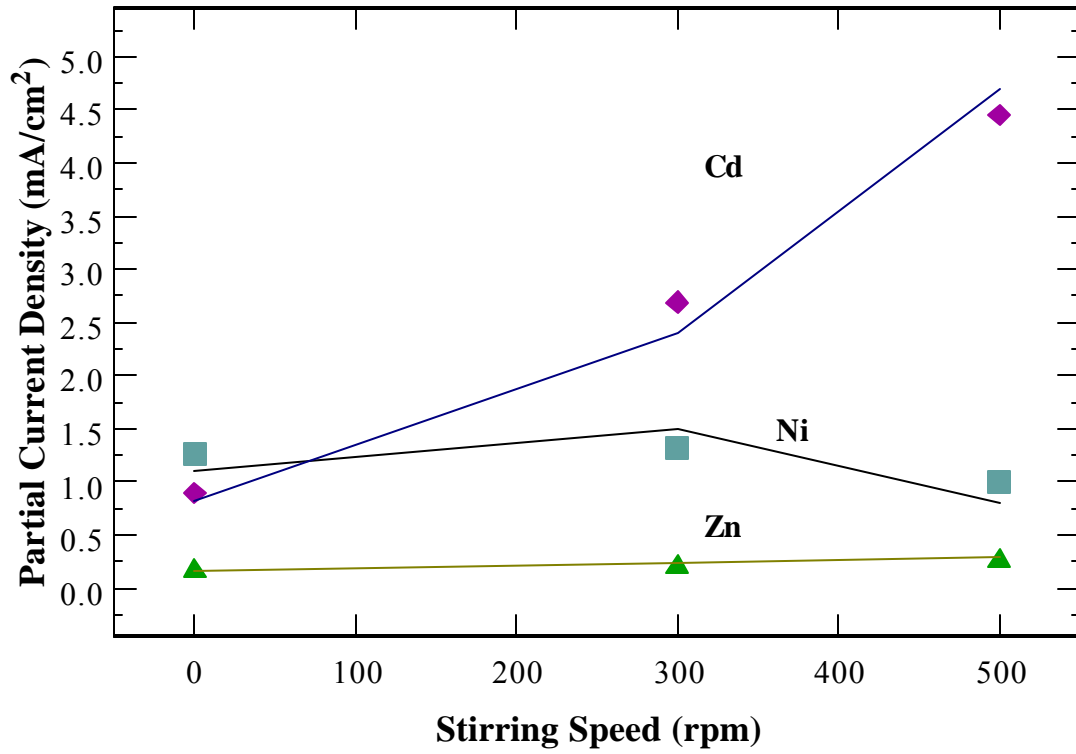


Fig. 7

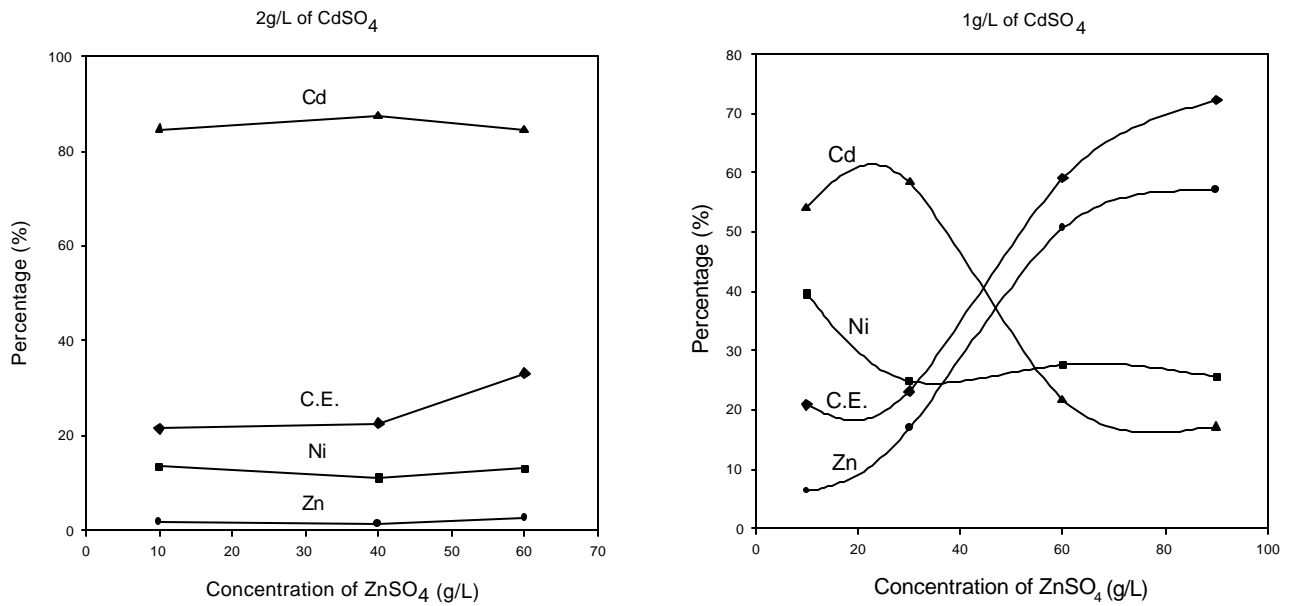


Fig. 8.

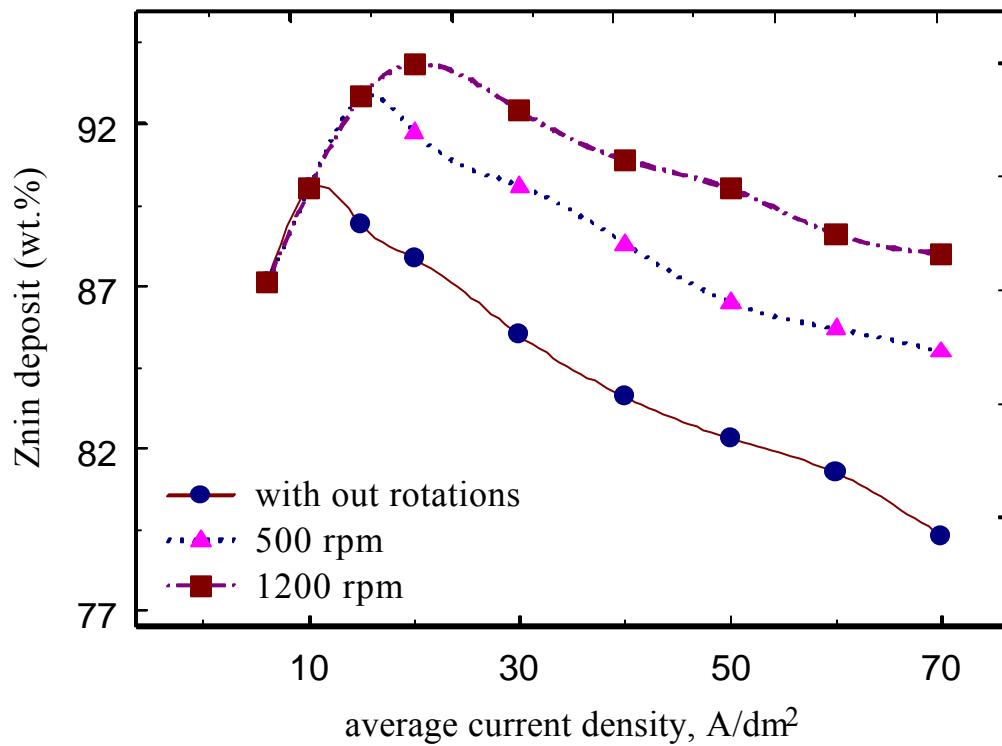


Fig 9

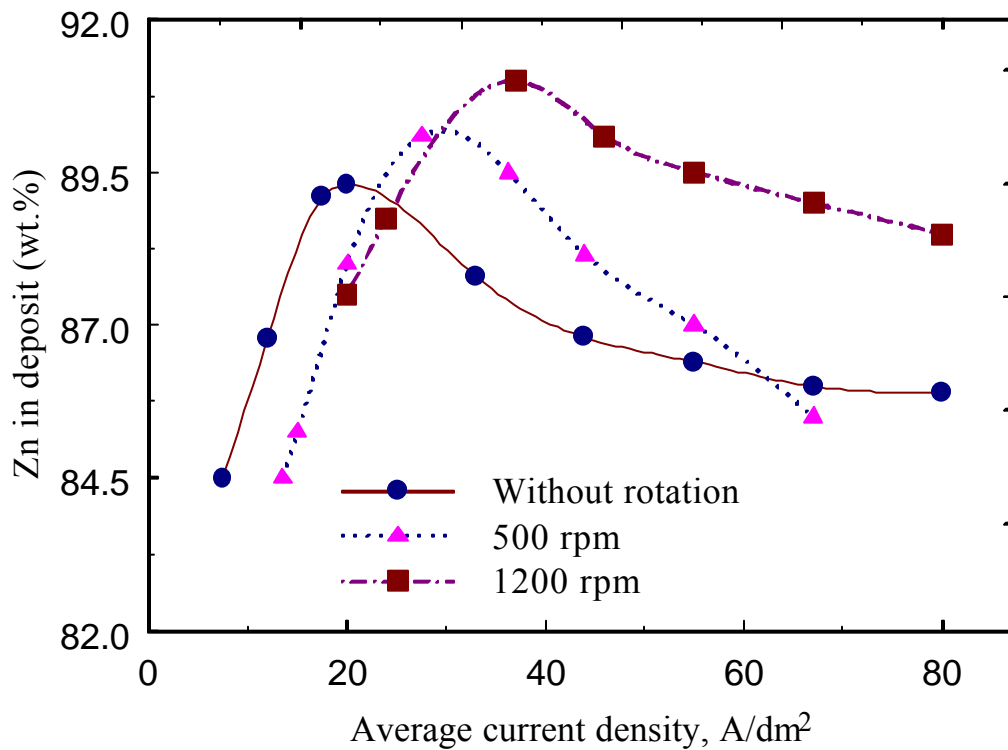


Fig 10

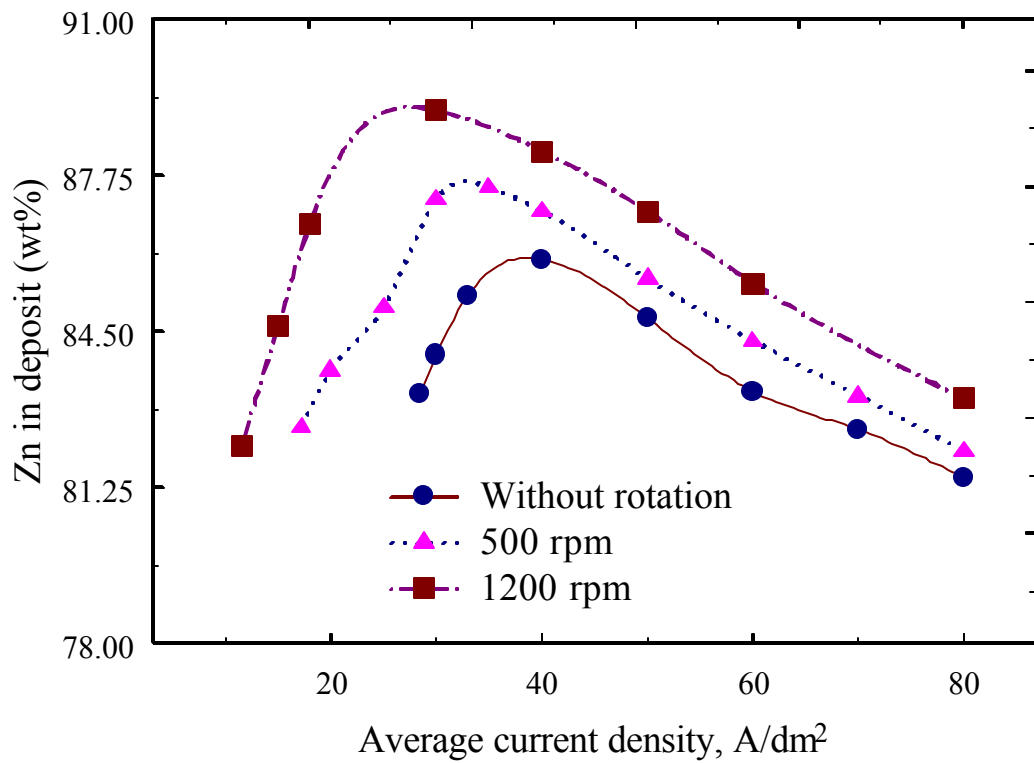


Fig 11